Discrimination of Muscovitisation Processes Using a Modified Quartz–Feldspar Diagram: Application to Beauvoir Greisens

Michel Cathelineau, Zia Steven Kahou

minerals

MDPI

Article

Discrimination of Muscovitisation Processes Using a Modified Quartz–Feldspar Diagram: Application to Beauvoir Greisens

Michel Cathelineau * and Zia Steven Kahou

Université de Lorraine, CNRS, GeoRessources, F-54000 Nancy, France; zia-steven.kahou@univ-lorraine.fr
* Correspondence: michel.cathelineau@univ-lorraine.fr

Abstract: Alteration in greisen-type granites develops through the progressive replacement of feldspars by potassic micas. Under the name 'greisen', quartz–muscovite assemblages display differences and include a variety of facies with variable relative proportions of quartz and muscovite. In principle, feldspar conversion to muscovite is written usually considering constant aluminium, and should result in a modal proportion of six quartz plus one muscovite. In Beauvoir greisens, which result from albite-rich granite, the relative proportion of quartz–muscovite is in favour of muscovite. Such a balance results from a reaction that implies imputs of potassium and aluminium, thus different from the classic one. The Q'-F' diagram provides a graphical solution for discriminating between reaction paths. A representative series of greisen data from the literature is compared in this diagram: Beauvoir B1 unit, Cligga Head, Cinovec, Panasqueira, Zhengchong, and Hoggar.

Keywords: greisen; muscovite; quartz; differentiated granites; chemical–mineralogical diagram

Citation: Cathelineau, M.; Kahou, Z.S. Discrimination of Muscovitisation Processes Using a Modified Quartz–Feldspar Diagram: Application to Beauvoir Greisens. *Minerals* **2024**, *14*, 746. https://doi.org/10.3390/min14080746

Academic Editors: Ignez de Pinho Guimarães and Jefferson Valdemiro De Lima

Received: 3 July 2024
Revised: 19 July 2024
Accepted: 22 July 2024
Published: 25 July 2024

1. Introduction

Rocks derived from granites containing only quartz and micas are often called 'greisen' without specifying the relative abundance of quartz and micas. The origin of the word greisen dates back to the Middle Ages (Saxonian miners), and greisens are nowadays considered as a rock composed mainly of quartz and micas, often zinnwaldite, but not systematically. These minerals are accompanied by other minor mineral phases such as topaz, tourmaline, and fluorite [1–4]. The word greisen is used for quartz–muscovite alterations affecting granitic rocks, most often leucocratic differentiated granites, rich in albite, derived from a peraluminous or metaluminous magmatic suite [4–8].

$$\begin{gathered} 3NaAlSi_3O_8 + K^+ + 2H^+ \leftrightarrow K(AlSi_3)(Al_2)O_{10}(OH)_2 + 3\,Na^+ + 6SiO_2 \\ 3\,Albite + K^+ + 2H^+ \leftrightarrow Muscovite + 3\,Na^+ + 6\,Quartz \end{gathered} \quad (1)$$

The most famous greisens are those from Cligga Head, which meet the strict definition of greisens composed of quartz and mica [8,9]. The most striking feature of the Cligga Head granite is the sharp drop in sodium content, which implies almost total conversion of albite to muscovite. In principle, the reactions that form the greisens at Cligga Head follow the typical hydrothermal reaction where a feldspar (potassic or sodic) is replaced by muscovite in a reaction written considering aluminium as constant. For albite-rich granite, the reaction would be written as follows:

There are many examples of peraluminous granites with the replacement of mainly albite or several feldspars (microcline and albite) by micas. Located in the north of the French Massif Central, the albite–lepidolite–topaz Beauvoir granite represents a fascinating case of mica development. During the 'hydrothermal greisen' phase (as defined by [10] and later by [11,12]), albite, which predominates in unaltered granite, K-feldspar, which displays a variable content in the Beauvoir intrusion, and a part of lepidolite are replaced by muscovite, which is considered to be hydrothermal. The 'greisens' defined at Beauvoir contain mainly muscovite-type micas [12,13], which add to or replace the abundant fraction

of phyllosilicates of magmatic origin, which occurs in the form of lepidolite at the Beauvoir B1 unit.

The albite–lepidolite–topaz Beauvoir granite represents an ideal evolved granite to study the evolution of micas and Li behaviour from the magmatic stage to the hydrothermal stage. It is located in the Sioule series of the northern French Massif Central [14]. At the Beauvoir B1 unit, lepidolite constitutes the main magmatic phyllosilicate, and its proportion is close to ~20 wt.%. During the hydrothermal greisen phase, feldspars (mostly albite) and lepidolite are replaced by hydrothermal muscovite [10,12]. Cuney et al. [10] consider that greisen from Beauvoir are "classical quartz-muscovite fissure type" and limited to the top of the Beauvoir B1 unit. Fonteilles [15] devotes a few lines to the greisen and considers that it contains muscovites I and II and sericites but does not provide a detailed description. Historical studies on the drill hole GPF-1 did not address the evolution of the relative quantities of quartz and muscovite to monitor the alteration. Moreover, only eight whole-rock analyses, mostly on fresh granites, are available on the first 200 m of the GPF drill hole, including only one sample with significant alteration [10,16]. However, these two studies carried out on the drill hole GPF-1 did not address the type of evolution of the relative quantities of quartz and muscovite as an indicator of the relative mobility of Si and Al in the vicinity of greisens.

However, an examination of the geochemical data for the greisenised Beauvoir granite showed some notable geochemical differences from other greisens. This prompted a graphical representation of the main mineral transformations to distinguish the different types of reactions and chemical balances involved in these alterations. The Q'-F' diagram [17], which breaks down the three main mineral poles of granites in the well-known quartz feldspar triangle (quartz, albite, and microcline), was used, taking into account the geochemical data for total rock as well as the crystallochemical data for the main granite-forming minerals and greisens. Significant differences emerged between the greisens from several localities prompting us also to consider data from the literature on several other well-known greisens such as those from Cligga Head [9], Cinovec (Germany-Czech Republic [6,7,18,19], Panasqueira (Portugal [5,20]), and others such as a greisen described in China in the region within the Shengdong batholith [21] and Hoggar [22].

2. Materials and Methods

2.1. Samples

Fresh granites and greisens were sampled for whole-rock analyses from three drill cores by Imerys in 2022 in the Beauvoir quarry (location map in Figure 1).

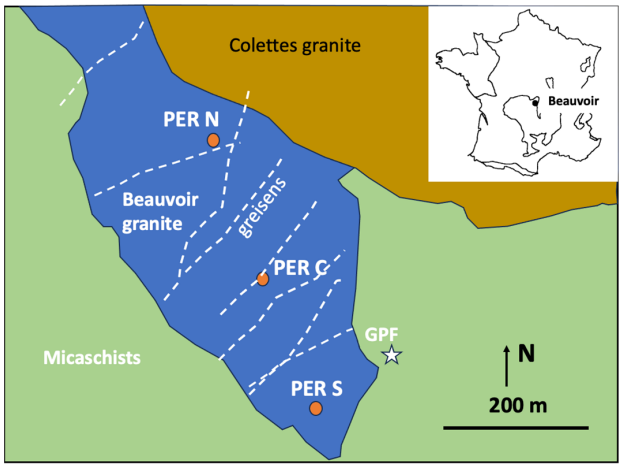

Figure 1. Location of the Beauvoir granite in the French Massif Central (inset) and location of the three studied drill holes (orange circles) from the Imerys 2022 campaign (PER N, C and S), and of the GPF deep drill hole.

2.2. Bulk Rock Analyses

Unaltered to altered granites were analysed in whole rock for significant elements. Whole-rock major and trace element analyses were performed on field samples at the Service d'Analyse des Roches et des Minéraux (SARM), Centre de Recherches Pétrographiques et Géochimiques (CRPG), Nancy, France. Major elements were analysed by inductively coupled plasma optical emission spectrometry on a Thermo-Fischer ICap 6500 173 instrument (Thermo Fisher Scientific, Waltham, MA, USA). Trace elements, including rare earth elements (REEs), were determined by inductively coupled plasma mass spectrometry (Thermo-Elemental X7, ESI, Omaha, NE, USA). Detailed analytical procedures are given in [23].

Bulk rock data on greisens from the literature for comparison are the following:

- Panasqueira: Two distinct granites are affected by greisens (partially greisenised G1, granite inferred as the main biotite granite) and pseudo-greisens affecting the G4 Rare Metal Granite from the cupola [6]. Two data sets are available: those from [6,20], which are mainly concerned with the cupola.
- Cinovec greisens occur as steep or flat zones of intensive metasomatic greisenisation along tens to hundreds of meters [7,24]. Feldspars are replaced by quartz, zinnwaldite, topaz, and fluorite. Cinovec granite geochemistry has been covered in numerous papers. However, the number of studies of greisens or greisenised granites is low. The authors of [6,7,18,25] have provided a series of whole-rock analyses on granites undergoing greisenisation. In greisen, zinnwaldite is re-equilibrated and then muscovitised [8].
- Cligga Head: Greisens conserve their granite texture and consist of quartz, protolithionite (inherited from the granite), muscovite, tourmaline, and topaz [8]. Hall [9] considers that quartz represents 52% (modal), muscovite 40%, tourmaline 5%, and topaz 0.8% of the greisen composition. The albite is entirely replaced by muscovite. Muscovite is already more abundant than protolithionite in the granite, but its abundance increases in the greisen, where protolithionite disappears [10]. Muscovites from greisen contain lithium around 2500 ppm Li_2O. A few whole-rock analyses are available in [10].
- In China, in the Zhengchong granite, several greisens were described by Liu et al. [21]. The greisen I is mainly composed of quartz (50%–55%), zinnwaldite (25%–30%), topaz (5%–10%), and fluorite (~5%). Greisen II exhibits a porphyritic-like texture where matrix and phenocrysts are observed. The matrix is mainly composed of quartz (45%–55%), zinnwaldite (15%–25%), topaz (10%–15%), and fluorite (~5%).
- In Hoggar, several greisens from the area Tamanrasset in the Pan-African Hoggar appear to result from two processes: the formation of quartz–topaz and quartz-rich greisens, followed by a quartz dissolution and its replacement by Li-rich micas, thus forming mica-rich greisens [22].

2.3. Method for Graphically Processing Geochemical Data: The Q'-F' Diagram

The chemical–mineralogical approach is based mainly on processing the analytical data for the major elements in a diagram that makes it easy to recognise the mineralogical significance of the chemical variations. It is based quantitatively on the chemical composition of the major elements analysed in bulk. It uses parametric processing of the data on the main chemical elements to reflect the actual mineralogy quickly and unambiguously, thus using 'chemo-mineralogical' diagrams in the same way as in [17,26,27].

The diagram (Figure 2) breaks down the locations of quartz, potassium feldspar, and plagioclase in a triangle close to the quartz–albite–potassium feldspar triangle [28]. Using the nomenclature of [28,29] for plutonic rocks, Debon and Lefort [27] have superimposed a new classification grid on this diagram. This diagram uses the two coordinates $Q' = Si/3 - (K + Na + 2\,Ca/3)$ and $F' = K - (Na + Ca)$ expressed in gram-atoms $\times 10^3$ of each element in 100 g of rock or mineral; the values used for the diagram are thus proportional to the molar contents of each element (see Table S1 in the Supplementary Materials for the detailed calculation). Q' is proportional to the quantity by weight of quartz in com-

mon granitoid rocks, as it corresponds to the silicon not linked to feldspars and muscovite. The Q′-F′ diagram (Q′ = Si/3 − (K + Na) versus F′ (K-Na)), modified by [17], eliminates variations in calcium content. This simplification is acceptable for hyperdifferentiated granites where most of the calcium is carried by apatite, as plagioclase is very close to albite and does not contribute to the calcium content. The Beauvoir granite, but also most of the other albitic peraluminous magmas, such as those of the Argemela intrusion [30], Segura [31,32] and references therein, which are similar to LCT pegmatites, have a calcium concentration monitored by apatite.

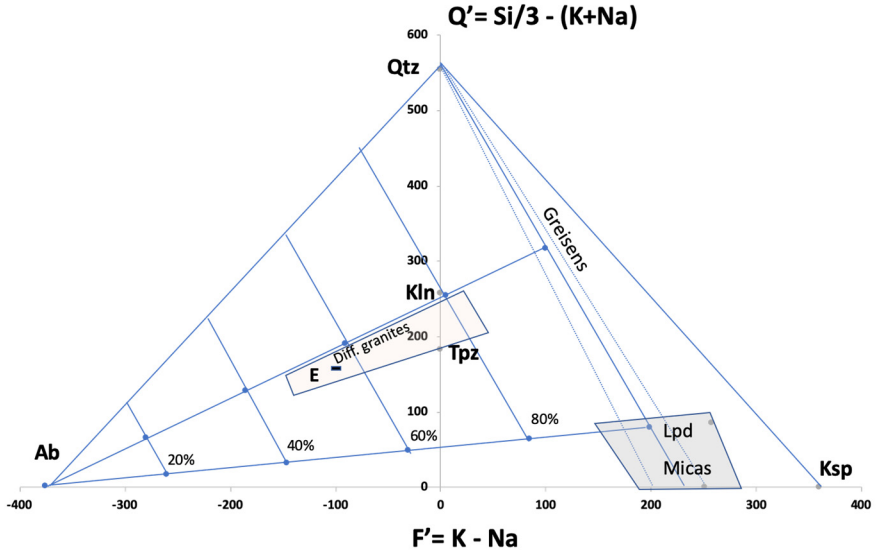

Figure 2. Principle of using the Q′-F′ diagram with the location of the main rock-forming minerals and the main alteration trend. Qtz: quartz; Kln: kaolinite; Toz: topaz; Lpd: lepidolite; Ab: albite; Ksp: K-feldspar; E (square): eutectic of the granite system by [33]. Diff. granites: differentiated granite field.

This diagram is well suited to the classification of felsic plutonic rocks. Still, it has already been used to represent alteration, particularly the dissolution of quartz associated with the crystallisation of potassic minerals [17]. The diagram helps discriminate between rocks composed of quartz and muscovite issued from the alteration in felsic rocks, particularly greisen. Note that the equidimensional aspect of the triangle is not respected when expanding the F′ axis to facilitate the reading of the greisen trends (see the following diagrams).

The main advantage of these chemical–mineralogical diagrams is that molar abundances are calculated, thus eliminating the effect of masses and allowing reactions between minerals to be represented as vectors whose slopes reflect the stoichiometry of reactions and structural formulae. Therefore, an albite–feldspar-K transformation is represented by a horizontal vector, and thus the transformation of albite into muscovite can be expressed—taking into account the assumptions concerning the constant element of the reaction—by vectors with well-defined and logical slopes.

3. Results

3.1. Mineralogical Analysis of Beauvoir Granite and Greisen

In the transition from fresh Beauvoir granite to greisen, the main mineral change is the replacement of albite with fine-grained muscovite. Thus, lepidolite is only of magmatic origin in the Beauvoir granite, and the newly formed micas, during later alteration, are muscovites. When present, the K-feldspar is also replaced in the most altered sample. However, the lepidolite is also replaced partially by muscovite. The shape and content of other minerals remain unchanged.

Composite and elemental maps using micro-X-ray fluorescence allowed us to determine quantitatively the relative mineral proportions [34] In the fresh sample, the mineralogy consists of albite (~45%), quartz (~25%), lepidolite (~20%), orthoclase (<10%), topaz and phosphates (<5%), and Sn-Nb-Ta oxides (<1%). In the altered facies, the feldspars tend to be replaced by hydrothermal muscovite and hydrothermal quartz. As a consequence, muscovite (~40%) and quartz (~40%) modal proportions increase while feldspars (<10%) and lepidolite (<~10%) proportions decrease.

The composition of lepidolite is relatively constant in fresh granite, and muscovite also has a well-defined composition, characterised by a very low Li content [12,13].The analyses of the two types of K-micas were also reported in the Q′-F′ diagram, where they form two very distinct clusters, both of which are aligned on the same quartz–mica line (Figure 3).

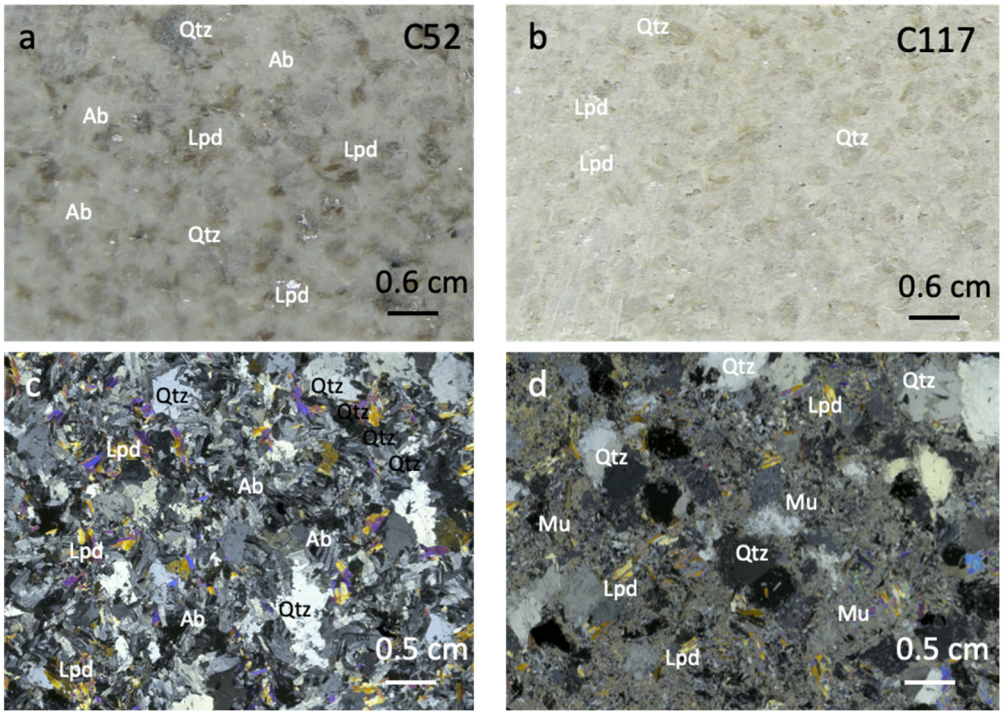

Figure 3. Petrography of the Beauvoir granite and related greisen from two samples collected from a drill hole realised in the central part of the Beauvoir quarry by Imerys (see Table 1 for whole-rock analyses). (**a**,**c**) fresh granite at 52 m depth, macroscopic view and corresponding thin section under crossed Nichols: coloured laths are lepidolites (Lpd), albite (Ab) is visible as elongated thin laths, and quartz (Qtz); (**b**,**d**) greisen at 117 m depth and corresponding thin section under crossed Nichols: albite is entirely replaced by fine-grained muscovite (Mu) and a part of the lepidolite is still visible as well as magmatic quartz. Fine-grained quartz is associated with fine-grained muscovite.

Table 1. Whole-rock analyses of representative samples of the Beauvoir granite (fresh, altered (muscovite-rich), and greisens). All numbers in %, except the two last lines, correspond to the calculated parameters Q′ and F′. Sample labels correspond to two distinct drill holes: C: centre; S: south; and numbers correspond to the depth in meters. Samples are presented classified at increasing values of the parameter F′.

Sample	**C123**	**C52**	**S113**	**C30**	**S58**	**C112**	**C39**	**C43**	**C42**	**S73**	**C117**
		Fresh Granites					**Altered Granites**			**Greisens**	
SiO_2	66.68	68.24	68.96	68.45	68.08	69.50	67.94	65.49	65.35	71.38	72.28
TiO_2	0.00	0.00	0.00	0.00	0.00	0.00	0.00	0.00	0.00	0.00	0.00
Al_2O_3	19.35	17.28	18.19	18.13	17.31	17.69	18.02	18.12	17.54	18.22	17.88

Table 1. *Cont.*

Sample	C123	C52	S113	C30	S58	C112	C39	C43	C42	S73	C117
			Fresh Granites					Altered Granites		Greisens	
Fe_2O_3	0.06	0,13	0.08	0.05	0.05	0.10	0.07	0.17	0.25	0.10	0.07
FeO	bdl	0.80	0.30	0.08	0.15	0.14	0.05	0.19	0.18	0.10	0.12
MnO	0.02	0.09	0.04	0.04	0.02	0.07	0.05	0.04	0.06	0.05	0.06
MgO	0.00	0.00	0.05	0.00	0.00	0.00	0.00	0.06	0.12	0.03	0.04
CaO	0.33	0.75	0.30	0.28	0.54	0.68	0.69	1.40	2.07	0.62	0.10
Na_2O	10.36	5.95	5.84	5.80	5.26	4.70	4.46	4.25	2.04	0.09	0.11
K_2O	0.90	1.95	2.70	2.90	3.60	3.33	3.23	3.28	4.00	5.40	5.89
P_2O_5	0.50	2.45	0.35	1.14	1.21	1.26	1.09	1.29	1.62	0.51	0.10
L.O.I.	1.22	2.85	2.39	2.45	2.53	2.50	3.26	3.84	5.67	3.27	2.97
F	0.44	2.18	1.95	2.39	1.67	1.92	2.50	2.68	2.03	1.00	0.87
Total	99.43	100.56	99.22	99.32	98.76	99.99	98.86	98.14	98.93	99.78	99.53
F′	−315.0	−150.5	−131.2	−125.4	−93.5	−81.0	−75.3	−67.7	19.1	111.8	121.6
Q′	16.6	145.3	136.7	131.1	131.4	163.2	164.4	156.5	211.7	278.4	272.4

3.2. Diagram Q′-F′ Applied to Granites and Greisens

3.2.1. Beauvoir Alteration Suite

Bulk-rock analyses of the Beauvoir granites and greisens are provided in Table 1. From unaltered albite-rich granites to profoundly altered and muscovite-rich granites, the main evolution of rock-forming major chemical elements is a progressive decrease in Na, correlatively to an increase in K. The unaltered granites and greisens of Beauvoir plotted in the Q′-F′ diagram, covering all the facies of progressive alteration identified in petrographic studies, so-called reference series, are distributed according to a trend line from the albite-rich granites to a point situated on the line joining quartz to lepidolite and muscovite. The trend is covered, and the most altered point is relatively well defined and confined to a relative proportion of 45% and 55% of quartz and micas, respectively.

The trend line for the representative series of samples (red dots in Figure 4) is as follows:

$$Q' = 0.579\ F' + 205.6 \qquad (R^2 = 0.97) \qquad (2)$$

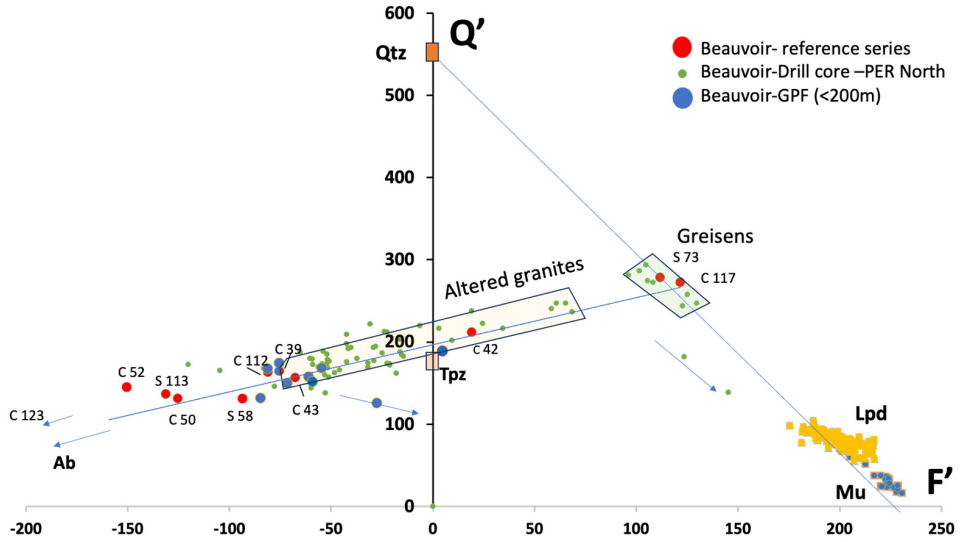

Figure 4. The Q′-F′ diagram applied to the Beauvoir granite to greisen series: in red, the reference samples are characterised by petrography and quantitative mineralogy; labels of red data points refer to the samples from Table 1 (drill holes PER C and S (centre and south), numbers: depth in meter); and in green, the data for drill cores from the northern area of the quarry (PER North). The GPF data, in blue circles, are from [16]. Lpd: lepidolite population from Beauvoir after [35]). Ab: albite' Tpz: topaz; Qtz: quartz; Lpd: lepidolite; and Mu: muscovite. Lepidolite and muscovite analyses from [34]. The blue arrows indicate enrichments in micas.

The northern zone of the Beauvoir quarry is the most affected by greisens. Using the analyses carried out on 4 m samples from the north of the borehole from the 2022 campaign (Imerys analyses), all the points converge towards the same point as the analyses of the reference series (Figure 4). Two exceptions concern a muscovite-rich structure enriched for which a displacement of the data points is observed in the direction of muscovite.

3.2.2. Panasqueira

At Panasqueira, most of the available data concern the greisens developed at the expense of the granite G4 (RMG) outcropping at the apex (cupola) of the main granite. A significant part of the greisens is distributed along the quartz–muscovite line, towards the intersection of the Beauvoir trend with the quartz–lepidolite + muscovite trend of Beauvoir, where three data points display similar compositions to the Beauvoir greisen. The Q′-F′ diagram, therefore, discriminates the greisenisation trend at Panasqueira from that of Beauvoir. In addition, a series of data points for greisens join the intersection with the quartz–muscovite line and the greisen from Beauvoir (orange arrow 'b' in Figure 5).

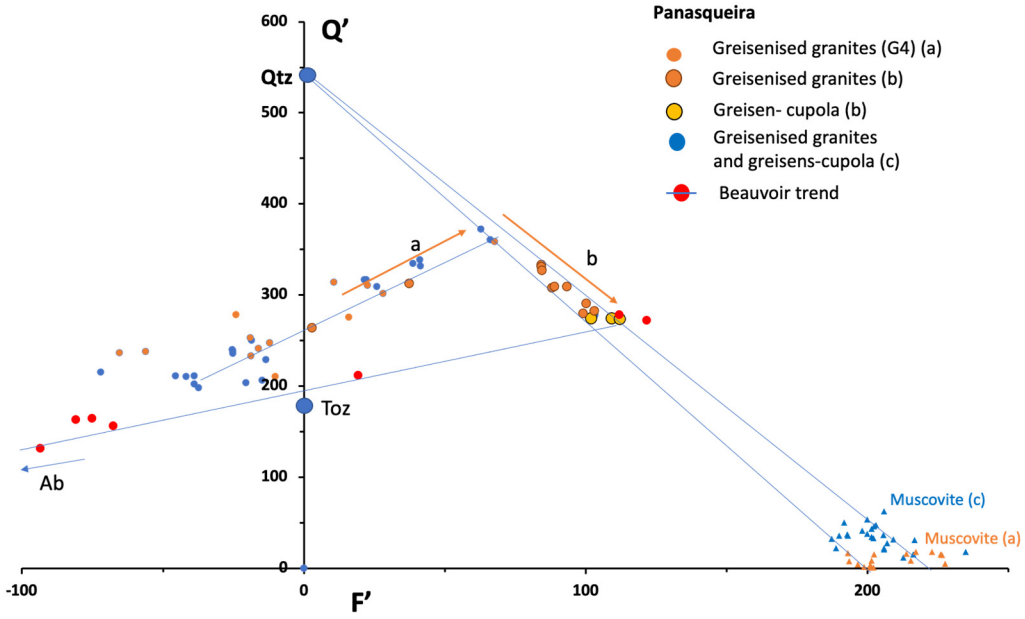

Figure 5. The Q′-F′ diagram applied to the Panasqueira granite to greisen series: in red, the reference samples characterised in petrography and quantitative mineralogy from Beauvoir; in orange and yellow (data noted a and b), respectively, from [6,36] compiled in Marignac et al. [6], and in blue (data noted c from [20]). Trend I corresponds to quartz–mica development, and trend II corresponds to quartz loss and further mica enrichment. Micas are indicated by triangles using the same colours as whole rock from the same two references (micas from greisenised G4 granite (noted a) [6]; micas from cupola greisen [20] (noted c)).

3.2.3. Other Examples

Cligga Head and Cinovec

Cligga Head altered granites, as a result of incipient greisenisation, follow a trend subparallel to that of Beauvoir granites. Greisens, however, do not plot precisely in the continuity of this trend but are displaced in the direction of quartz from the intersection of this trend with the quartz–muscovite line (Figure 6).

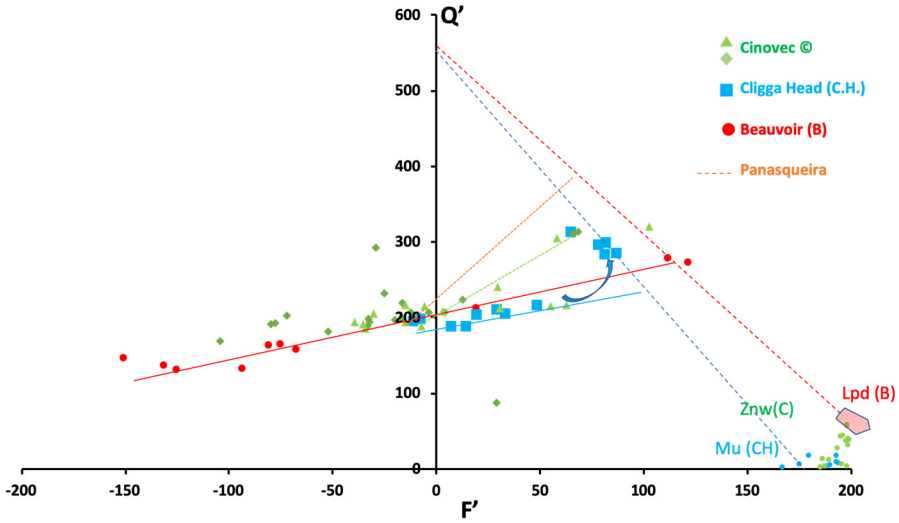

Figure 6. The Q′-F′ diagram applied to the Cligga Head (CH, data from [9]) and Cinovec (C, data from [6,7,25]) granite to greisen series. The trend for Beauvoir whole-rock analyses is red (in pink, Beauvoir (noted B) lepidolite (Lpd)). Muscovite data are sourced from the same literature references as for the whole-rock analyses (Znw: zinnwaldite from Cinovec [8]; Mu: muscovites from Cligga Head [9]).

For Cinovec, the number of analyses of intermediate facies between granites and the corresponding greisens is low. Four data points are distributed around the trend obtained for Cligga Head and Beauvoir. Considering the three data points on greisens, they display similar features to those of Cligga Head, e.g., a displacement towards quartz from the intersection between the alteration trend and the quartz–zinnwaldite line (Figure 6).

The Zhengchong and Hoggar Greisens

In the Zongsheng granite, greisens are rich in topaz but plot in an intermediate domain, similar to that described for Cligga Head greisens. Data points are somewhat dispersed and do not follow clear evolutions (Figure 7).

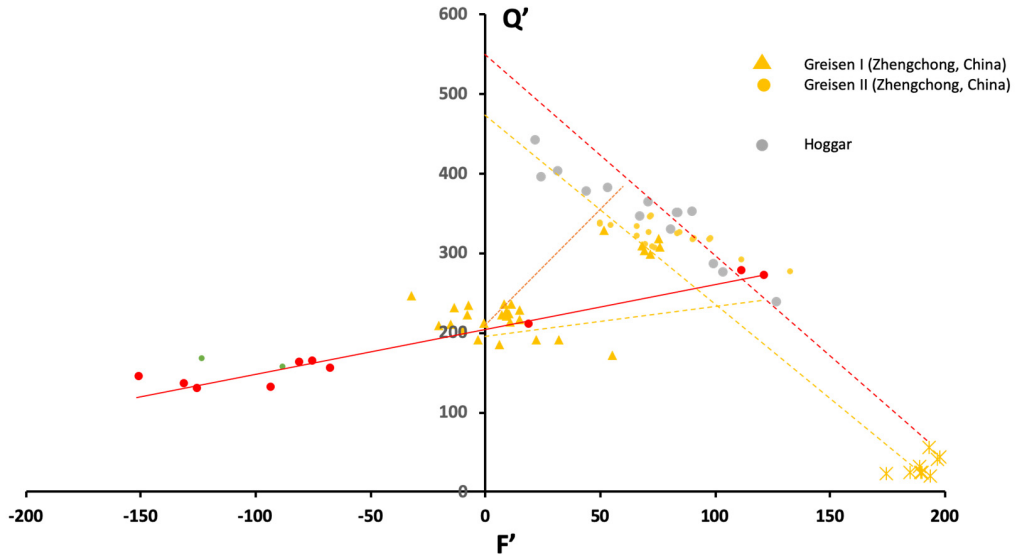

Figure 7. The Q′-F′ diagram applied to the Zengchong (China, data from [21] in yellow) and Hoggar (in grey, data from [22]) granite to greisen series. Yellow stars correspond to mica analyses from [21] for Zenchong greisens. In red are the Beauvoir data points and their reference line for comparison.

Most of the samples from Hoggar greisens are characterised by a richness in quartz and a trend that follows the quartz–muscovite line in the direction of quartz. There is no clear evidence of the impact of quartz dissolution on bulk chemistry as most data points remain within the field described in all other mentioned examples, except for one data point slightly enriched in micas (Figure 7).

4. Discussion

4.1. Main Trend for the Beauvoir Granite

The primary trend corresponds to a trend from an albite-rich pole on the one hand to another pole characterised by enrichment in quartz and lepidolite. The first trend may be considered magmatic in origin and may correspond to different amounts of albite respective to lepidolite due to probable magmatic segregation among minerals.

In continuity with the magmatic trend, the alteration trend with a similar slope characterises the altered facies, where muscovite replaces mostly albite and lepidolite in the most extreme degrees of alteration. The above values are around Q' = 150, corresponding to F' = −80, and the points continue to line up on the same axis. Still, petrography indicates that points correspond to a significant albite replacement by a quartz–muscovite mixture. The quartz–muscovite amount increases to the greisen, but the relative amount of quartz versus phyllosilicates (lepidolite + muscovite) remains the same. The intersection of this trend with the quartz (lepidolite–muscovite) line corresponds to a rock constituted of around 40% quartz and 60% phyllosilicates. This trend does not correspond to a feldspar replacement trend at constant Al as would be expected in a greisen, which is a reaction generally written at constant Al for K-feldspar muscovitisation, as aluminium is typically not considered mobile at the hydrothermal stage:

$$3\ KAlSi_3O_8 + 2H^+ \leftrightarrow K(AlSi_3)(Al_2)O_{10}(OH)_2 + 2K^+ + 6SiO_2 \quad (3)$$

$$K - feldspar + 2H^+ \leftrightarrow Muscovite + 2K^+ + 6SiO_2$$

Here, the trend may be explained from the point of view of the bulk mass balance by roughly replacing albite with quartz and mica in similar amounts. Such relative amounts of quartz and K-micas pose problems concerning the mass balance of aluminium, which, in that case, cannot be considered constant.

The slope found for Beauvoir samples is relatively close to the theoretical slope defined by the following equation:

$$\begin{gathered} 2\ NaAlSi_3O_8 + K^+ + Al^{3+} + 2\ H_2O \\ \leftrightarrow K(AlSi_3)(Al_2)O_{10}(OH)_2 + 3\ SiO_2 + 2\ H^+ + 2Na^+ \end{gathered} \quad (4)$$

$$2\ Albite + K^+ + Al^{3+} + 2H_2O \ \leftrightarrow Muscovite + 3\ Quartz + 2\ H^+ + 2Na^+$$

which is an equal combination of two other equations written either at constant Si or, more traditionally, at constant Al (the classical equation proposed for greisens),

$$3\ NaAlSi_3O_8 + K^+ + 2H^+ \leftrightarrow K(AlSi_3)(Al_2)O_{10}(OH)_2 + 6SiO_2 + 3Na^+ \quad (5)$$

$$3\ Albite + K^+ + 2H^+ \leftrightarrow Muscovite + 6\ Quartz + 3\ Na^+$$

(constant Al, greisen equation),

$$NaAlSi_3O_8 + K^+ + 2Al^{3+} + 4H_2O \leftrightarrow K(AlSi_3)(Al_2)O_{10}(OH)_2 + 6H^+ + Na^+ \quad (6)$$

$$Albite + K^+ + 2Al^{3+} + 4H_2O \leftrightarrow Muscovite + 6H^+ + Na^+$$

(constant Si).

The resulting trend is noted as 'A' in Figure 8.

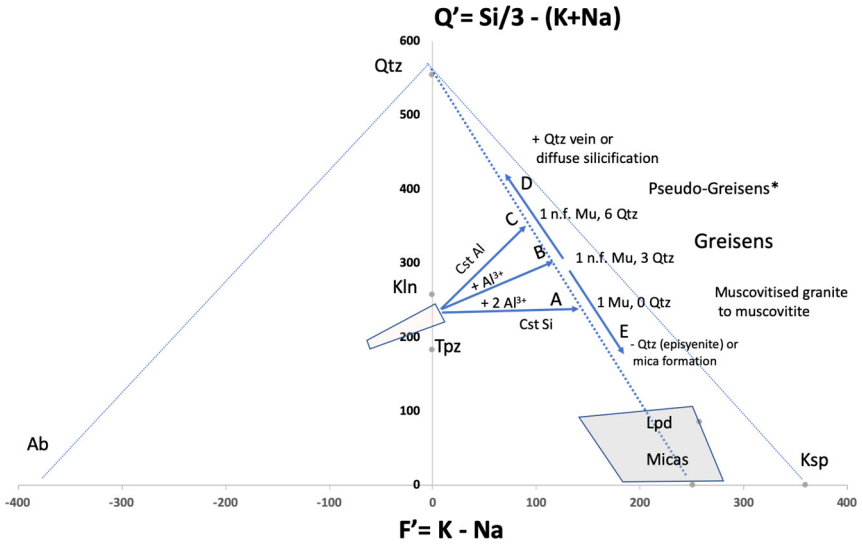

Figure 8. The Q′-F′ diagram with the main alteration trends depending on the mobility of aluminium with three vectors: A: at constant Si (Cst Si); B: with the addition of one Al^{3+}, consisting of a combination of A (constant Si) and C (at constant Al); and additional processes such as quartz precipitation (D) or quartz dissolution and replacement by micas (E). *: Pseudo-greisens as defined by [6,22] as silicified granite, then dequartzified partially with quartz replacement by muscovite. n.f. Mu: newly formed muscovite; Qtz: quartz; and Lpd: lepidolite.

4.2. Differences among the Other Greisen Examples

The trends of progressive greisenisation are relatively complete at Beauvoir between fresh and altered granites. They differ significantly from those obtained for Panasqueira granites, for which the trend also almost continues towards the quartz–mica line with all intermediate compositions. It has, however, a slope distinct from that of Beauvoir. It falls onto the line of the conversion of feldspars to muscovite following Equations (3) and (4), thus with a mass balance produced by a constant aluminium reaction (trend 'B' in Figure 8).

The trends obtained at Cinovec and Cligga Head are very similar to those of Beauvoir for the first increment of greisenisation (trend 'A'). Greisens, however, are slightly displaced towards a composition more enriched in quartz and intermediate than the intersection between the greisen trend and the quartz–muscovite line, but without reaching the greisen line produced by a reaction at constant Al.

The trend obtained from Hoggar data is unclear and does not offer intermediate terms. The greisen trend reveals variable quartz contents covering greisens enriched in quartz–topaz and a muscovite greisen that are not very different from the Beauvoir greisen in composition. Both are not significantly enriched in muscovite.

The main differences between all the rocks, so-called 'greisens', concern the nature of the inherited undissolved minerals from the granite, the nature of the newly formed minerals, and the behaviour of silicon. Phyllosilicates differ, but most are muscovites, except for Cinovec, where the zinnwaldite is considered recrystallised, and muscovite late and not linked to greisenisation [7]. At Beauvoir, topaz is already present in the fresh granite, and no further newly formed topaz is identified in the greisen facies. On the contrary, topaz is linked to the greisen stage at Cligga Head and is accompanied by tourmaline and fluorite [9].

4.3. Aluminium Mobility and Muscovite Development

Many experimental works have emphasised aluminium mobility at temperatures higher than 400 °C. The richness in F, Li, and sometimes B could explain specific complexation and Al mobility in peraluminous granites ([35,37] and references therein) and porphyry–granite systems [38]. If Equation (3) represents the Beauvoir trend, it requires a contribution of potassium and aluminium from the fluid to replace the albite with mus-

covite. It generates two times less quartz, explaining the location of the greisens closer to the muscovite pole than the greisens from Panasqueira.

It is, however, rather difficult to identify the causes of the different trends as detailed fluid chemistry is not available. In most cases, fluids as fluid inclusions are most aqueous with low-density volatile components. The presence of high amounts of fluorine is an essential factor to consider. Burt [39] proposed two main greisenisation routes: (a) systems at high temperature (>500 °C) and relatively low pressure, where hydrothermal brines demix, thus separating a vapour phase rich in volatiles (HF and HCl) that are highly aggressive and responsible for the mica formation, and (b) greisens formed at lower temperatures (250 to 500 °C) but higher pressure without boiling. For Tagirov and Schott [40], in the case of a fluid initially containing 0.01 m of fluorine at 450 °C-1 kbar, a high mobility of Al occurs due to the formation of mixed Na-Al-O-H-F complexes. Then, during greisenisation, if the topaz precipitates, Al passes into the form of $Al(OH)^{-}$ and $NaAl(OH)^{0}$ to the detriment of the hydroxide fluoride species. The dissolution capacity of the fluid consequently decreases, and the Al mobility falls. Finally, Tagirov and Schott [41] suggest that Al-Si and Al-OH species are responsible for transporting Al in acid solutions circulating in lower-temperature hydrothermal veins, which could be the case for the Beauvoir greisens that formed along fractures. In all cases, aluminium is mobile, and its transport is facilitated by fluorine.

In the specific case of Beauvoir, the acidic fluids have been channelised within a network of fractures. These fluids, probably issued from the unmixing from the magmatic melts as suggested by [42] and confirmed by [40], were in significant disequilibrium with the granite mineral assemblage due to their richness in fluorine and pH. Albite was primarily dissolved and replaced by newly formed muscovite. The preferential dissolution of albite and its replacement by K-micas is also the main trend at Cligga Head and Cinovec. The main difference at Beauvoir is the relatively small amounts of K-feldspar in the parent granite. The amount of potassium released by the muscovitisation of K-feldspars is insufficient to account for the need for potassium. Another deficit concerns aluminium. The albite dissolution may have provided a part of the local aluminium, but another contribution is probably the transported aluminium in the solution. The origin of the aluminium contribution can be either minerals from the granite itself along the fractures or the surrounding schists, which are known to have been deeply affected by hydrothermal reaction with recrystallisation of the original metamorphic micas [10–12,43].

An overall summary of the major changes occurring among the main rock-forming minerals is proposed in Figure 9, where processes identified at Beauvoir are compared to the other considered greisens. A distinction is made between early greisens directly related to the magmatic fluid release and the greisens formed along fractures during later stages. The latter are dominated mainly by K-micas, which are close to the muscovite end-member.

4.4. Silicification in the Granite Mass or Quartz Dissolution and Quartz Vein Formation

The location along the quartz–muscovite line depends mainly on the relative abundance of newly formed quartz and muscovite during greisenisation but also on later processes such as fracture reactivation and formation of quartz vein infillings, or conversely of quartz dissolution and eventual conversion of quartz to muscovite through this process. This is the hypothesis from [5] for Panasqueira and [22] for Hoggar greisens. The suggested mechanism is a substitution of feldspar by quartz (silicification), followed by quartz dissolution (episyenite) and mica crystallisation. Such silicification processes have also been reported by [41] for porphyry–greisen alteration. In addition, at Beauvoir, fluids from the greisen stage occured at the end of the process, and quartz precipitation as veinlets, which contribute to vein-type silicification, is probably linked to cooling. Veins are highly abundant in the northern zone.

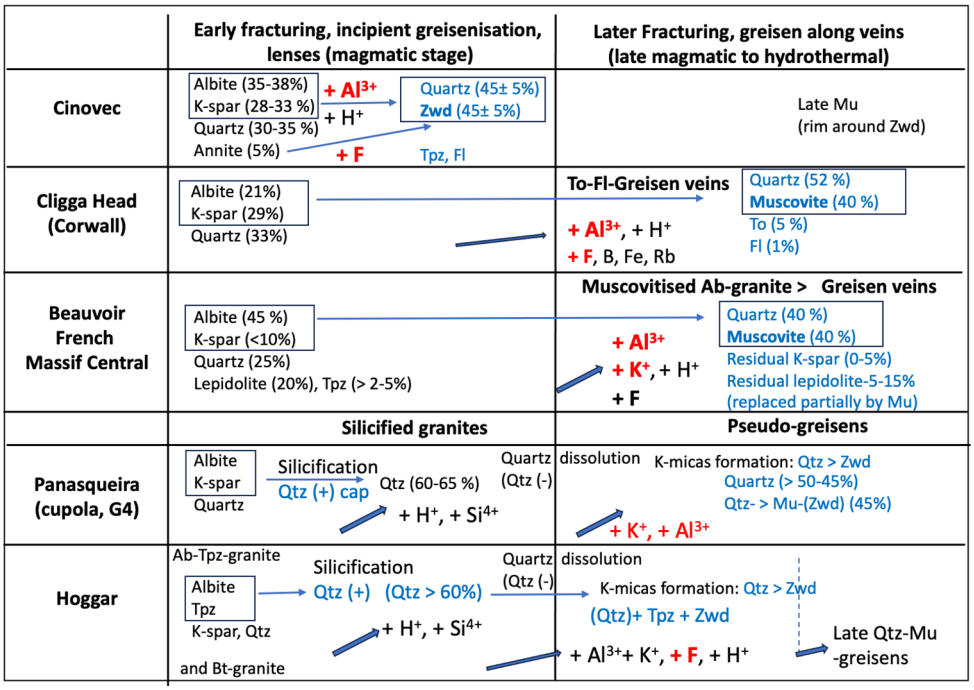

Figure 9. Summary of the main mineral reactions and transformations related to the examined greisen types. The main element supplies needed for the transformations are put forward. Zwd: zinnwaldite; Mu: muscovite; Mu(Zwd) muscovite–zinnwaldite series; Tpz: topaz; Qtz: quartz; and Fl: fluorite. Data have been simplified and summarised from the literature, except Beauvoir (Cinovec [6,7], Cligga Head [9], Panasqueira [5,20], and Hoggar [22]).

5. Conclusions

Major chemical element concentrations obtained by whole-rock chemical analyses are rich in informations and are indicative of the mass balance occurring during greisenisation. These chemical elements provide helpful information on the main trends of water–rock interactions. Aluminium appears mobile, although it is generally considered immobile in most mass balance calculations. The main trends obtained on several greisens, including Beauvoir granite, indicate that the chemical reaction usually written at constant aluminium cannot explain the slope of many trends in the quartz–feldspar–mica system. Aluminium has a specific mobility, which can be explained by acidic fluids containing fluorine.

Mineralogical specificities of each greisen testify to a distinct succession of mineral dissolution and mineral saturation depending on the fluid chemistry and temperature evolution.

In the specific case of Beauvoir, a network of fractures channelled fluids that were in significant disequilibrium with the mineral assemblage of the granite, particularly albite, and, owing to the aluminium transported, formed a substantial quantity of muscovite. The origin of the aluminium and potassium necessary for these reactions can be either minerals from the granite itself along the fractures or the surrounding schists, which are known to have been deeply affected by hydrothermal reaction with recrystallisation of the original metamorphic micas.

Supplementary Materials: The following supporting information can be downloaded at https://www.mdpi.com/article/10.3390/min14080746/s1. Table S1: Bulk-rock analyses of granites and greisens with Q′-F′ parameter calculations.

Author Contributions: M.C.: sampling, data acquisition and interpretation, conceptualisation, writing (original draft preparation, review and editing), and funding acquisition; Z.S.K.: sampling, analytical data, interpretation, writing (review and editing), and funding acquisition. All authors have read and agreed to the published version of the manuscript.

Funding: This research was funded by Labex Ressources21 under the reference ANR-10-LABX-21-RESSOURCES21, supported by the Agence Nationale de la Recherche through the national programme "Investissements d'avenir and by Imerys through the collaboration programme between UL and Imerys".

Data Availability Statement: Data are partly provided in this paper. Data from Imerys are not publicly available due to ownership by Imerys.

Acknowledgments: O. Rouer and A. Lecomte (GeoRessources) are warmly acknowledged for their help in acquiring the EMPA and SEM-EDS data. M-C Boiron is acknowledged for her help in reading drafts and proofs. Imerys is warmly acknowledged for providing geochemical data and samples for the present study, particularly G. Jean, P. Fullenwarth, and B. Barré, for their fruitful discussions. Two anonymous reviewers are thanked for their constructive remarks.

Conflicts of Interest: The authors declare no conflicts of interest.

References

1. Černý, P.; Masau, M.; Goad, B.E.; Ferreira, K. The Greer Lake leucogranite, Manitoba, and the origin of lepidolite-subtype granitic pegmatites. *Lithos* **2005**, *80*, 305–321. [CrossRef]
2. Černý, P.; Blevin, P.L.; Cuney, M.; London, D. Granite-related ore deposits. *Econ. Geol.* **2005**, *100*, 37–370.
3. Shcherba, G.N. Greisens. *Int. Geol. Rev.* **1970**, *12*, 114–150. [CrossRef]
4. Štemprok, M. Greisenization (a review). *Geol. Rundsch. Stuttg.* **1987**, *76*, 169–175. [CrossRef]
5. Marignac, C.; Cuney, M.; Cathelineau, M.; Lecomte, A.; Carocci, E.; Pinto, F. The Panasqueira rare metal granite suites and their involvement in the genesis of the world-class Panasqueira W-Sn-Cu vein deposit: A petrographic, mineralogical, and geochemical study. *Minerals* **2020**, *10*, 562. [CrossRef]
6. Breiter, K.; Ďurišová, J.; Hrstka, T.; Korbelová, Z.; Vaňková, M.H.; Galiova, M.V.; Kanicky, V.; Rambousek, P.; Knesl, I.; Dobes, P.; et al. Assessment of magmatic vs. metasomatic processes in rare-metal granites: A case study of the Cínovec/Zinnwald Sn–W–Li deposit, Central Europe. *Lithos* **2017**, *292–293*, 198–217. [CrossRef]
7. Breiter, K.; Hložková, M.; Korbelová, Z.; Galiová, M.V. Diversity of lithium mica compositions in mineralised granite-greisen system: Cínovec Li-Sn-W deposit, Erzgebirge. *Ore Geol. Rev.* **2019**, *106*, 12–27. [CrossRef]
8. Charoy, B. Greisenisation, minéralisation et fluides associés à Cligga Head, Cornwall (Sud-ouest de l'Angleterre). *Bull. Mineral.* **1979**, *102*, 633–641. [CrossRef]
9. Hall, A. Greisenisation in granite of Cligga Head, Cornwall. *Proc. Geol. Assoc.* **1971**, *82*, 209–230. [CrossRef]
10. Cuney, M.; Marignac, C.; Weisbrod, A. The Beauvoir topaz-lepidolite albite granite (Massif Central, France); the disseminated magmatic Sn–Li–Ta–Nb–Be mineralisation. *Econ. Geol.* **1992**, *87*, 1766–1794. [CrossRef]
11. Monnier, L.; Salvi, S.; Jourdan, V.; Sall, S.; Bailly, L.; Melleton, J.; Béziat, D. Contrasting fluid behavior during two styles of greisen alteration leading to distinct wolframite mineralisations: The Echassières district (Massif Central, France). *Ore Geol. Rev.* **2020**, *124*, 103648. [CrossRef]
12. Monnier, L.; Salvi, S.; Melleton, J.; Lach, P.; Pochon, A.; Bailly, L.; Béziat, D.; Parseval, P.D. Mica trace-element signatures: Highlighting superimposed W-Sn mineralisations and fluid sources. *Chem. Geol.* **2022**, *600*, 120866. [CrossRef]
13. Monier, G.; Charoy, B.; Cuney, M.; Ohnenstetter, D.; Robert, J.L. Évolution spatiale et temporelle de la composition des micas du granite albitique a topaze-lepidolite de Beauvoir. *Geol. Fr.* **1987**, *2–3*, 179–188.
14. Do Couto, D.; Faure, M.; Augier, R.; Cocherie, A.; Rossi, P.; Li, X.-H.; Lin, W. Monazite U–Th–Pb EPMA and zircon U–Pb SIMS chronological constraints on the tectonic, metamorphic, and thermal events in the inner part of the Variscan orogen, example from the Sioule series, French Massif Central. *Int. J. Earth Sci.* **2016**, *105*, 557–579. [CrossRef]
15. Fonteilles, M. La composition chimique des micas lithinifères (et autres minéraux) des granites d'Echassières comme image de leur évolution magmatique. *Geol. Fr.* **1987**, *2–3*, 149–178.
16. Rossi, P.; Autran, A.; Azencott, C.; Burnol, L.; Cuney, M.; Johan, V.; Kosakevitch, A.; Ohnenstetter, D.; Monier, G.; Piantone, P.; et al. Logs pétrographique et géochimique du granite de Beauvoir dans le sondage "échassieres I" Minéralogie et géochimie comparées. *Géol. Fr.* **1987**, *2–3*, 111–135.
17. Cathelineau, M. The hydrothermal alkali metasomatism effects on granitic rocks: Quartz dissolution and related subsolidus changes. *J. Petrol.* **1986**, *27*, 945–965. [CrossRef]
18. Štemprok, M. Drill hole CS-1 penetrating the Cínovec/Zinnwald granite cupola (Czech Republic): An A-type granite with important hydrothermal mineralisation. *J. Geosci.* **2016**, *61*, 395–423. [CrossRef]
19. Hreus, S.; Výravský, J.; Cempírek, J.; Breiter, K.; Galiová, M.V.; Krátký, O.; Šešulka, V.; Skoda, R. Scandium distribution in the world-class Li-Sn-W Cínovec greisen-type deposit: Result of a complex magmatic to hydrothermal evolution, implications for scandium valorisation. *Ore Geol. Rev.* **2021**, *139*, 104433. [CrossRef]
20. Launay, G.; Sizaret, S.; Lach, P.; Melleton, J.; Gloaguen, E.; Poujol, M. Genetic relationship between greisenization and Sn-W mineralisations in vein and greisen deposits: Insights from the Panasqueira deposit (Portugal). *Bull. Soc. Geol. Fr.* **2021**, *192*, 2. [CrossRef]

21. Liu, C.; Xiao, W.; Zhang, L.; Belousova, E.; Rushmer, T.; Xie, F. Formation of Li-Rb-Cs greisen-type deposit in Zhengchong, Jiuyishan district, South China: Constraints from whole-rock and mineral geochemistry. *Geochemistry* **2021**, *81*, 125796. [CrossRef]
22. Bouguebrine, J.; Bouabsa, L.; Marignac, C. Greisen and pseudo-greisen in the Tamanrasset area (Central Hoggar, Algeria): Petrography, geochemistry and insight on the fluid origin from mica chemistry. *J. Afr. Earth Sci.* **2023**, *202*, 104898. [CrossRef]
23. Carignan, J.; Hild, P.; Mevelle, G.; Morel, J.; Yeghicheyan, D. Routine analyses of trace elements in geological samples using flow injection and low pressure on line liquid chromatography coupled to ICP-MS: A study of geochemical reference material BR, DR-N, EB-N, AN-G and GH. *Geostand. Newsl.* **2001**, *25*, 187–198. [CrossRef]
24. Johan, Z.; Strnad, L.; Johan, V. Evolution of the Cínovec (Zinnwald) granite cupola, Czech Republic: Composition of feldspars and micas, a clue to the origin of W, Sn mineralisation. *Can. Mineral.* **2012**, *50*, 1131–1148. [CrossRef]
25. Stemprok, M.; Sulcek, Z. Geochemical Profile through an Ore-Bearing Lithium Granite. *Econ. Geol.* **1969**, *64*, 392–404. [CrossRef]
26. La Roche, H. Sur l'usage du concept d'association minérale dans l'étude chimique des roches: Modèles chimiques, statistiques, représentations graphiques, classification chimico minéralogique. *C.R. Acad. Sci. Paris* **1966**, *262*, 1665–1668.
27. Debon, F.; Le Fort, P.A. Cationic classification of common plutonic rocks and their magmatic associations: Principles, method, applications. *Bull. Minéralogie* **1988**, *111*, 493–510. [CrossRef]
28. Streckeisen, A.L. Classification and nomenclature of plutonic rocks. *Geol. Rundsch.* **1974**, *63*, 773–786. [CrossRef]
29. Streckeisen, A.L. Classification of the common igneous rocks by means of their chemical composition. *Neues Jahrb Miner. Monatsh* **1976**, *1*, 1–15.
30. Michaud, J.A.S.; Pichavant, M. Magmatic fractionation and the magmatic-hydrothermal transition in rare metal granites: Evidence from Argemela (central Portugal). *Geochim. Cosmochim. Acta* **2020**, *289*, 130–157. [CrossRef]
31. Antunes, I.M.; Neiva, A.M.; Ramos, J.M.; Silva, P.B.; Silva, M.M.; Corfu, F. Petrogenetic links between lepidolite-subtype aplite-pegmatite, aplite veins and associated granites at Segura (Central Portugal). *Geochemistry* **2013**, *73*, 323–341. [CrossRef]
32. Cathelineau, M.; Boiron, M.C.; Leconte, A.; Martins, I.; Dias da Silva, I.; Mateus, A. Lithium, phosphorus, fluorine-rich intrusions and the phosphate sequence at Segura (Portugal): A comparison with other hyper-differentiated magmas. *Minerals* **2024**, *14*, 287. [CrossRef]
33. Tuttle, O.F.; Bowen, N.L. Origin of granite in the light of experimental studies in the system $NaAlSi_3O_8$-$KAlSi_3O_8$-SiO_2-H_2O. *Geol. Soc. Am.* **1958**, *74*, 153.
34. Kahou, S.; Cathelineau, M.; Boiron, M.-C. Quantitative mineralogy and lithium distribution in the upper part of the Beauvoir granite. In Proceedings of the EGU24-2024, Vienna, Austria, 14–19 April 2024. 1668-ECS, Orals, GMPV5.1.
35. Gresens, R.L. Composition-volume relationships of metasomatism. *Chem. Geol.* **1967**, *2*, 47–55. [CrossRef]
36. Pinto, F.M.V. ICP-MS Data of the SCB2 Drill-Hole. Beiralt Tin and Wolfram (Portugal) Data. Beiralt Tin and Wolfram (Portugal) Mining Company; *Unpublished Report*, 2016.
37. Errandonea-Martin, J.; Garate-Olave, I.; Roda-Robles, E.; Cardoso-Fernandes, J.; Lima, A.; Ribeiro, M.A.; Teodoro, A.C. Metasomatic effect of Li-bearing aplite-pegmatites on psammitic and pelitic metasediments: Geochemical constraints on critical raw material exploration at the Fregeneda–Almendra Pegmatite Field (Spain and Portugal). *Ore Geol. Rev.* **2022**, *150*, 105155. [CrossRef]
38. Lentz, D.R.; Gregoire, C. Petrology and mass-balance constraints on major-, trace-, and rare-earth-element mobility in porphyry-greisen alteration associated with the epizonal True Hill granite, southwestern New Brunswick, Canada. *J. Geochem. Explor.* **1995**, *52*, 303–331. [CrossRef]
39. Burt, D.M. Acidity-salinity diagrams–Application to greisen and porphyry deposits. *Econ. Geol.* **1981**, *76*, 832–843. [CrossRef]
40. Harlaux, M.; Mercadier, J.; Bonzi, W.M.E.; Kremer, V.; Marignac, C. Geochemical signature of magmatic-hydrothermal fluids exsolved from the Beauvoir rare-metal granite (Massif Central, France): Insights from LA-ICPMS analysis of primary fluid inclusions. *Geofluids* **2017**, *2017*, 1925817. [CrossRef]
41. Tagirov, B.; Schott, J. Aluminum speciation in crustal fluids revisited. *Geochim. Cosmochim. Acta* **2001**, *65*, 3965–3992. [CrossRef]
42. Aissa, M.; Weisbrod, A.; Marignac, C. Chemical and thermodynamic characteristics of hydrothermal fluid circulation at Echassieres. *Geol. Fr.* **1987**, *2–3*, 335–350.
43. Aubert, G. Les coupoles granitiques de Montebras et d'Echassières (Massif central français) et la genèse de leurs minéralisations en étain, lithium, tungstène et béryllium. *Éditions BRGM* **1969**, *46*, 1.